Food Analytical Methods
https://doi.org/10.1007/s12161-022-02287-2

Quality Assessment of Tindora (*Coccinia indica*) Using Poincare Plot and Cartesian Quadrant Analysis

Tanmay Sarkar[1] · Alok Mukherjee[2] · Kingshuk Chatterjee[2] · Saule Ospandiyarovna Akhmetova[3] · Aigul Surapovna Alipbekova[4] · Marina Temerbayeva[5] · Mohammad Ali Shariati[6] · Maksim Rebezov[6,7] · Jose Manuel Lorenzo[8,9]

Received: 28 March 2022 / Accepted: 3 April 2022

Abstract

Tindora or ivy gourd (*Coccinia indica*) is a tropical vegetable and has the potential to become popular worldwide due to its rich nutritional characteristics, adaptability to adverse environmental condition and fast fruiting nature. The fresh samples are bright green (good) in colour; it turns yellow (intermediate quality) and ultimately turns bright red (bad or inedible as vegetable). In this paper, tindora is classified using two different colour representations of the image matrix, namely RGB and HSV. In the RGB representation, intensity of the green layer versus intensity of the red layer for each pixel position is plotted. The shape of the plot enables us to identify the tindora quality. In the case of HSV representation, the hue layer is used for classification purposes. The hue layer matrix is vectorized and the Poincare plot is computed. The distribution of the Poincare plot is analysed using Cartesian quadrant system. Based on the analysis, tindora quality is determined. The accuracy of the tindora classification using RGB representation is 68.67 and HSV representation is 94.33. The classifier used in both the representations after feature extraction is primarily threshold based and hence has low computational burden. The low computational burden makes the method ideal for incorporation into smartphones in the form of an app.

Keywords Vegetables · Food quality inspection · Artificial intelligence · Image analysis

Tanmay Sarkar and Alok Mukherjee contributed equally to this work.

✉ Tanmay Sarkar
tanmays468@gmail.com

✉ Jose Manuel Lorenzo
jmlorenzo@ceteca.net

Mohammad Ali Shariati
shariatymohammadali@gmail.com

Maksim Rebezov
rebezov@yandex.ru

[1] Department of Food Processing Technology, Malda Polytechnic, West Bengal State Council of Technical Education, Government of West Bengal, Malda 732102, India

[2] Government College of Engineering and Ceramic Technology, Kolkata, India

[3] Department of Chemistry, Chemical Engineering and Ecology, Almaty Technological University, 100 Tole Bi Str., Almaty 050012, Republic of Kazakhstan

[4] S. D. Asfendiyarov Kazakh National Medical University, 94 Tole Bi Str., Almaty 050012, Republic of Kazakhstan

[5] Faculty of Engineering and Technology, Innovative University of Eurasia, 45 Lomova Str., Pavlodar 140000, Republic of Kazakhstan

[6] Department of Scientific Research, K.G. Razumovsky Moscow State University of Technologies and Management (The First Cossack University), 73 Zemlyanoy Val, Moscow 109004, Russian Federation

[7] Department of Scientific Research, V. M. Gorbatov Federal Research Center for Food Systems, 26 Talalikhina Str., Moscow 109316, Russian Federation

[8] Centro Tecnológico de La Carne de Galicia, Avd. Galicia No. 4, Parque Tecnológico de Galicia, San Cibrao das Viñas, 32900 Ourense, Spain

[9] Área de Tecnología de los Alimentos, Facultad de Ciencias de Ourense, Universidade de Vigo, 32004 Ourense, Spain

Published online: 14 April 2022

Introduction

Vegetables are one of the important sources of nutrient for human health. It is rich in vital minerals, vitamins, other phytochemicals and dietary fibre. The deficiencies in micronutrient consumption are known as hidden hunger and are a serious problem throughout the world and most prominent in underdeveloped and developing countries. Iron (Fe), iodine (I) and vitamin A deficiencies are the major challenges that affect 2–3.5 billion people (Pfeiffer and McClafferty 2007). Owing to the fact of all these rich nutrients available in vegetables, consumption of this can reduce health risk to some extent. Proper amount of vegetables in daily diet can be a heal to vision-related problems, diabetes, gastrointestinal health, heart attack and stroke (Hossain and Maitra 2021). The recommended daily intake for vegetables is 200–250 g/day (Agudo 2005). It has been reported that lower amount of vegetables in daily diet can increase the rate of ischaemic heart disease by 31% while chances of stroke is increased by 11%. The bioactive compounds present in vegetables are able to modify metabolic activation, free radical scavenging and carcinogen detoxification (Wargovich 2000; Lalji et al. 2018). Alteration in diet may prevent gastrointestinal malignancies by 20–30% and 5–12% of all other types of carcinoma formation incidences (Dias 2011).

Owing to increase in the buying capacity of consumers, improved understanding of nutritional advantages and a craving for a variety of vegetables is rising. Customers, on the other hand, are becoming increasingly concerned about the food safety aspect. The modern marketing practices are replacing the traditional marketing not only in developed countries also in developing countries (Dias 2011). The criteria for procurement and quality management system in international marketing, long-distance shipping, supermarkets and numerous packaging and processing units are based on diversity of product, quality and safety issues and constant supply of product (Dias 2011; Singh 2021; Yuniarti et al. 2022). Farmers and small-scale industries are facing difficulties to meet the quality standard set by the modern marketing facilities. Thus efficient technology and efficiency to supply best-quality products with economic viability is essential at the farmers' end.

Coccinia indica (tindora) is a plant belonging from the botanical family Cucurbitaceae. The tropical vine is known as scarlet gourd or ivy gourd and native to Indian subcontinent. It is available widely in Australia, Tropical Asian countries, Southern America and Eastern Africa (Tamilselvan et al. 2011). The plant can sustain in prolonged drought condition, growth is rapid (up to 10 cm/day), and lower maintenance is required thus suitable in this era of global environmental change. The green tindora fruits (thick skinned, oval shaped, 5–6-cm long and 1.5–3.5-mm diameter) are consumed as vegetable (Gunjan et al. 2021). The juicy fruit has bitter aftertaste in raw condition, but with maturity the crunchy texture changes to softer one and the outer skin changes from green to orange or red. But the appearance of orange to red hue resembles with the deterioration of its quality as a vegetable. The vegetable has a shelf-life of 7–9 days in ambient environment. From ancient time, it is used in traditional medicine like Ayurveda and Unani as anti-diabetic, anti-inflammatory agent and medicine for scabies, small pox and ringworms (Sakharkar and Chauhan 2017; Bhaskar and Varma 2021). For maintenance of healthy endocrine system, the fruit is beneficial. It is composed of 3.1–3.4% carbohydrate, very less amount of fat (0.1–0.2%) and 1.2–1.4% of protein (Deokate and Khadabadi 2012; Alagarraja et al. 2017). It is a good source of minerals like calcium (40 mg/100 g), iron (1.4 mg/100 g) and phosphorus (30 mg/100 g) (Khatun et al. 2012). Apart from these, it is a potential source of phytochemicals like phenolic acids, flavonoids, vitamins and glycosides (Hadi et al. 2022).

For local marketing and export trading, it is becoming essential to grade the agricultural commodities, particularly vegetables. Vegetables are typically graded based on external attributes such as shape, size, weight, specific gravity and visual colour. The established techniques of evaluating vegetables for fresh marketing are machine grading and hand grading; size and shape are the basis of evaluation in both procedures. Healthy veggies should be graded according to their maturity, colour, shape, weight and size, while damaged and/or bruised vegetables should be sorted out. The classes I (extra fancy), II (superior) and III (standard) are the common classes in which the vegetables are graded. The manual gradation of vegetables has been carried out by skilled labours/experts considering the different pre-defined parameters for grading. But the process is labour extensive, time-consuming, cost extensive, erratic and tedious. Most of the vegetables are seasonal; thus in peak season, scarcity in manpower may hamper the post-harvest management and supply chain. Highly efficient grading system is a prerequisite in modern marketing trend; thus, efficient vegetable grading system is in demand in order to overcome the demerits of manual grading system. Size, weight, shape, rotating screen, reflectance and colour-based grading systems are available for different vegetables (Londhe et al. 2013). The artificial vision system or the digital image analysis mimic the human vision system electronically for quality inspection of the vegetables by identification, recognition and interpretation of the digital images captured (Table 1) (Sarkar et al. 2022). The mathematically perceived array of information is ultimately structured to construct a model for efficient vegetable

Table 1 Digital image analysis–based vegetable gradation systems

Vegetable	Input feature considered	Technique	Data set	Accuracy (%)	Reference
Potato	RGB	ANN	240 images	92	Przybylak et al. (2020)
	Colour, depth and enhanced depth images	CNN	7084 images; 297 potatoes	86.6	Su et al. (2020)
	Depth image	Linear regression	110 potatoes	88–90	Su et al. (2018)
Onion	Edge detection of X-ray images	ANN	400 onions	90	Shahin et al. (2002)
Eggplant	RGB	KNN	100 eggplant	88	Akter and Rahman (2017)
	RGB, HSV	Binarization, region of interest detection	-	-	Kondo et al. (2013)
Tomato	Shape and colour	BPNN	53 images	92	Kaur et al. (2018)
	Texture, colour and shape related 24 features	SVM	2666 tomatoes	97.74	Dhakshina Kumar et al. (2020)
Field peas	Colour, shape and size	Linear discriminant analysis	175 peas	97	McDonald et al. (2016)
Chilli	Colour	CNN	-	86	Hing et al. (2021)
	-	CNN	1200 images, 400 chilli	93.89	Hendrawan et al. (2021)
Capsicum	RGB, lab, XYZ	Discriminant analysis	-	81–100	Ropelewska and Szwejda-Grzybowska (2021)
Broccoli	RGB, HS	PNN	320 broccoli	93.4	Tu et al. (2007)
		ResNet	506 images	87.9	Zhou et al. (2020)
Carrot	RGB	Bayes classifier	600 carrots	88.3–95.5	Deng et al. (2017)
	-	CNN	878 carrots	99.43	Jahanbakhshi et al. (2021)
Okra or lady's finger	-	ResNet50	3200 images	99	Raikar et al. (2020)
Radish	RGB	Principle component analysis	-	95.2–97.1	Iwata et al. (1998)
Cabbage	Luminance information	Statistical analysis	99 images	-	Arce-Lopera et al. (2013)
Spinach	HSV, lab	SVM, ANN	100 spinach, 1045 images	70–84	Koyama et al. (2021)
Lettuce		CNN	160 lettuce	83–86	Cavallo et al. (2018)
Artichoke	RGB, area	Image segmentation		-	Otoya and Gardini (2021)
Sweet potato	Roundness, length, width	Statistical analysis	250 sweet potatoes	-	Boyette and Tsirnikas (2017)
Asparagus	Geometric, colour and shape (1931 features in total)	Neural network	955 images	90.2	Donis-González and Guyer (2016)

gradation (Bhargava and Bansal 2021). For image acquisition, smartphone is becoming a cheap and more feasible alternative; researchers have developed the smartphone-based artificial vision system for quality inspection of Indian gooseberry (Mukherjee et al. 2021, 2022b; Sarkar et al. 2021a), oyster mushroom (Sarkar et al. 2021b) and seafoods (Navotas et al. 2018; Hu et al. 2020).

There are a number of techniques available that can reliably predict the quality of fruits and vegetables. The supervised learning algorithms such as support vector machine (SVM), artificial neural network (ANN) and their modified versions involve complex mathematical analysis. Other methods such as fuzzy logic, wavelet transformation (WT), principal component analysis (PCA) and entropy analysis have heavy computational burden despite their excellent accuracy (Valous et al. 2009; Baranowski et al. 2012; Li et al. 2018; Rong et al. 2019; Koyama et al. 2021; Mukherjee et al. 2022c). Scholars are working to achieve similar levels of accuracy using approaches which are computationally light. Classification using Poincare plots is one such endeavour: primarily, Poincare plots are used to analyse biomedical signals (Mourot et al. 2004; Guzik et al. 2006; Hoshi et al. 2013). In this paper, the Poincare plot is used in food quality evaluation.

The Poincare plot investigates the interdependence of data points of a single signal and looks for any differences in the monotonic variation of the sample points. The correlation coefficient between each of the components is then computed. These correlation coefficients are then carefully examined to

determine the intensity level of each quality class, and a threshold-based classifier is designed.

Materials and Methods

Sample Collection

In total, 600 samples were collected from Birbhum and Malda districts of West Bengal, India, from the 2nd week of August 2021 to the 3rd week of September 2021. The tindora vegetable is elliptical in shape (length: 4.5–6.0 cm, diameter: 1.5–2.0 cm). The samples were collected after 48 h of flowering; the fresh samples were green coloured with white longitudinal mottling and with crunchy texture. However, the samples become yellow with time, and the full mature samples were red in colour and cannot be consumed as vegetable, and the texture becomes softer.

Image Acquisition and Assignment of Quality Class

The image acquisition and class assignment were conducted as per our previous work (Sarkar et al. 2021a, 2022; Mukherjee et al. 2022c, b). From the 600 samples, a dataset of 540 samples were developed by random selection method. Eighty samples were considered for training for each of the three classes (good, intermediate, bad), while a set of 100 samples were considered for the purpose of testing the proposed model.

RGB Representation–Based Classification

In this work, an attempt has been made to develop classification scheme for the detection of quality of tindora samples. We have observed that the vegetable samples are all green in colour while they are at the freshest most condition. The samples are kept aside as these develop yellow pigments as time progresses. This yellow colouring of the green tindora samples especially occurs from one of the edges of the sample, and this yellow colouring expands gradually towards the central part of the sample. With further progression of time, this yellow colouring gradually turns more towards the red spectrum. Thus, it has been concluded that the freshest sample is more greenish and the colour spectrum of the vegetable turns more towards the red zone as the sample turns old. The intermediate samples, however, show prominent tinges of combination of green, yellow as well as red to some extent. Figures 1 and 2 describe, respectively, a few random samples of images and the cropped images of three different quality classes along the central axis of the tindora samples. These figures further emphasize the development and

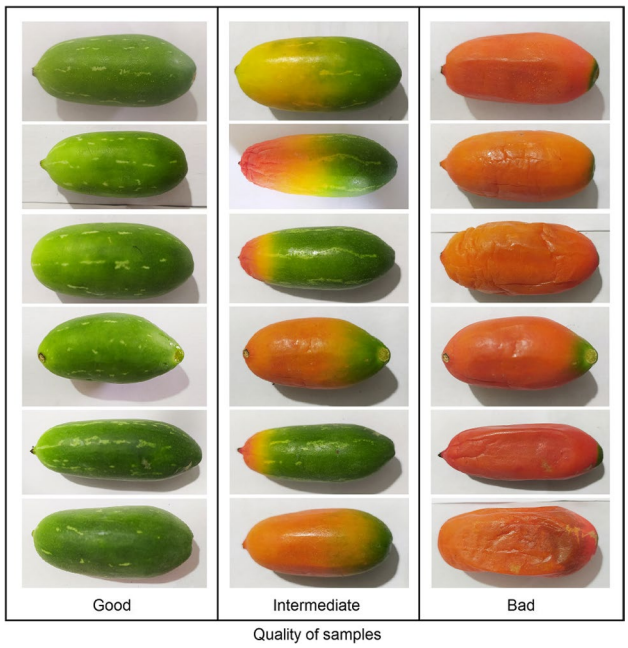

Fig. 1 Samples of images of the tindora samples taken at random

modification of colour of the tindora samples as these gradually rotten.

Thus, the red and the green layers of the samples can be analysed to estimate the concentration of red and green colours in the vegetables, respectively. Hence, the red and the green layers of the vegetable samples have been analysed, as well as the interrelation between these two layers have been computed. It is well observable from the images of the samples, as well as from the patches chosen near the central axis of the samples, as shown in Fig. 1, that the concentration of green tinge gradually fades as the vegetable turns rotten; on the contrary, the concentration of red tinge becomes higher as a sample turns old. Thus the following methods have been considered for the estimation of red and green concentration among the samples:

The average intensity of green tinge has been computed directly. In order to do that, the pixel intensity values of the entire image have been summed up, row-wise and column-wise. Finally, the summed intensity has been added along the row and along the columns to obtain a single value of the sum of intensity values of the overall image. Finally, this summed intensity value has been divided by the dimension of the image, which is 100×600, i.e. by 60,000, to obtain the mean pixel intensity level for the green layer. This mean level is actually representing the entire image. This mean pixel intensity level is denoted henceforth as the green intensity index in this work. Figure 3 represents the diagrammatic view of the methodology adopted in this work.

The red intensity level of the RGB colour map is also performed in a similar way using the red layer. Thereby, a

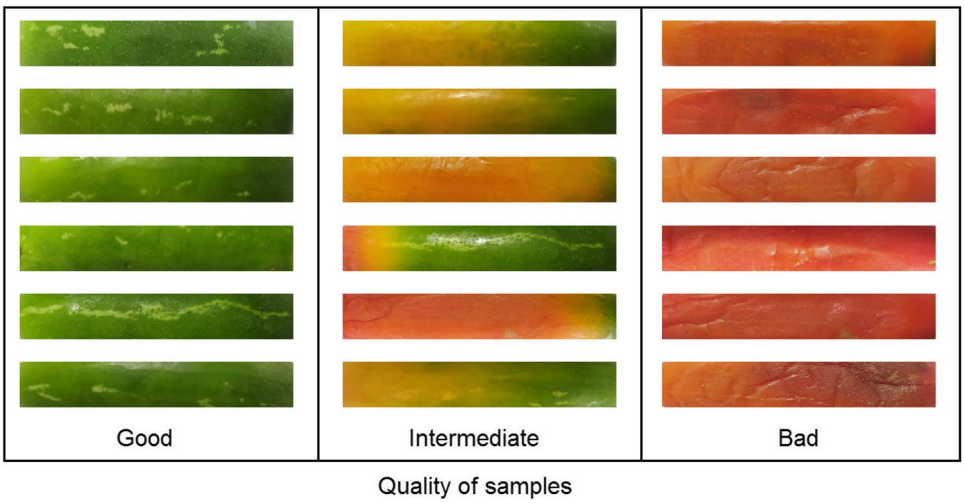

Fig. 2 Samples of cropped images of the tindora samples along the central axis taken at random

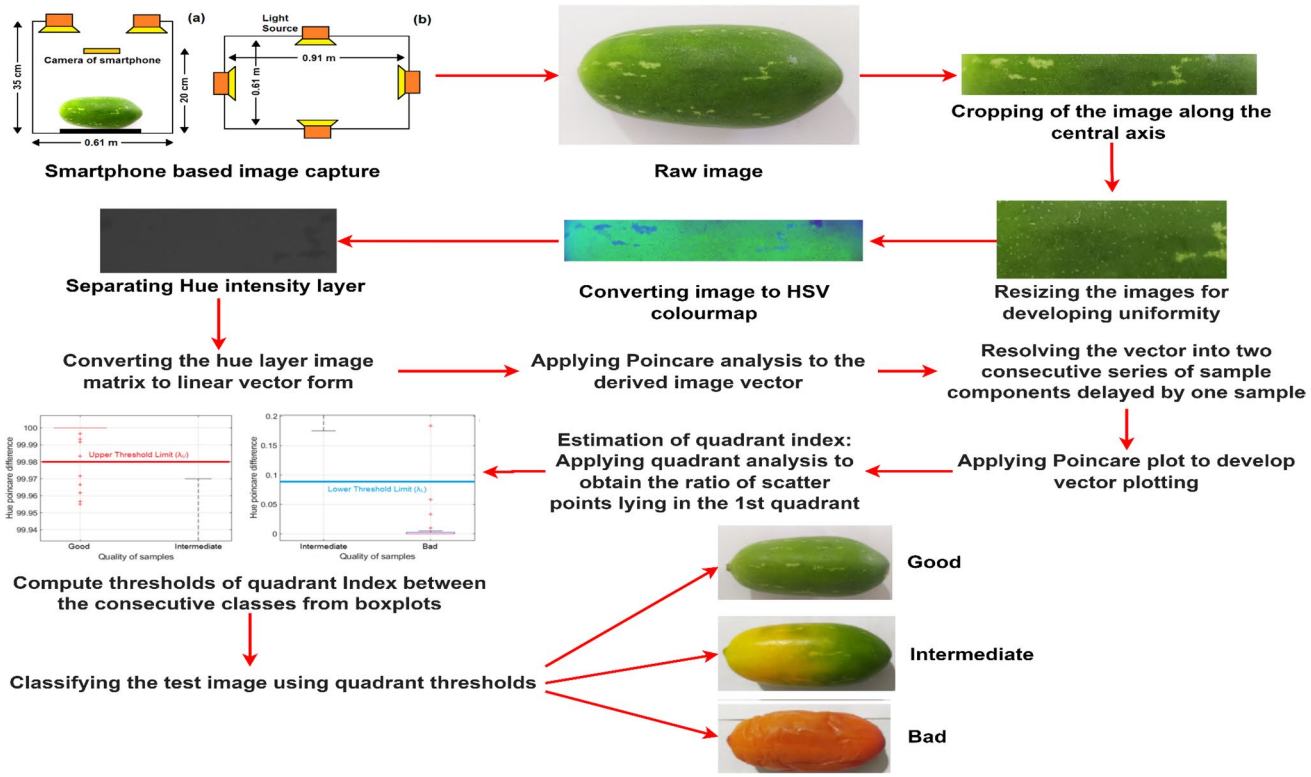

Fig. 3 The schematic representation of the proposed methodology adopted

similar red intensity index illustrating the mean pixel density of the red layer has been obtained. The mean pixel intensity levels for the green and red layers of a random set of samples are illustrated in Figs. 4 and 5, respectively.

In order to extract any feature regarding the interrelationship between the green and red layers, the intensity values of these two layers have been plotted as the two axis of 2D graph. The 100×600 image pixel intensity levels of the red and green channels have been plotted along the x-axis and y-axis, respectively, to obtain the 2D red-green intensity map indicating the interrelationship of these two colour components among the vegetable samples. Randomly selected few of these plots are shown in Figs. 6, 7 and 8, to represent the *good*, *intermediate* and *bad* class of samples, respectively.

Close observation of Figs. 6 to 8 reveals that there is sudden change in patterns of the red-green 2D plot as the samples transform from good quality to bad

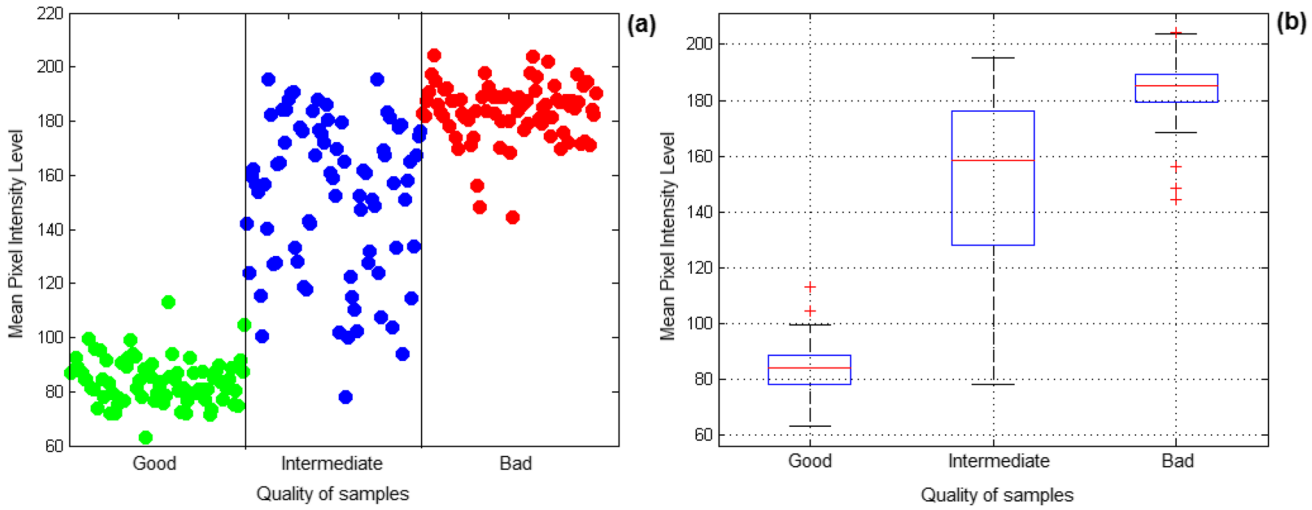

Fig. 4 Mean pixel intensity levels of red layer of the training tindora samples represented as **a** scatter diagram and **b** boxplot

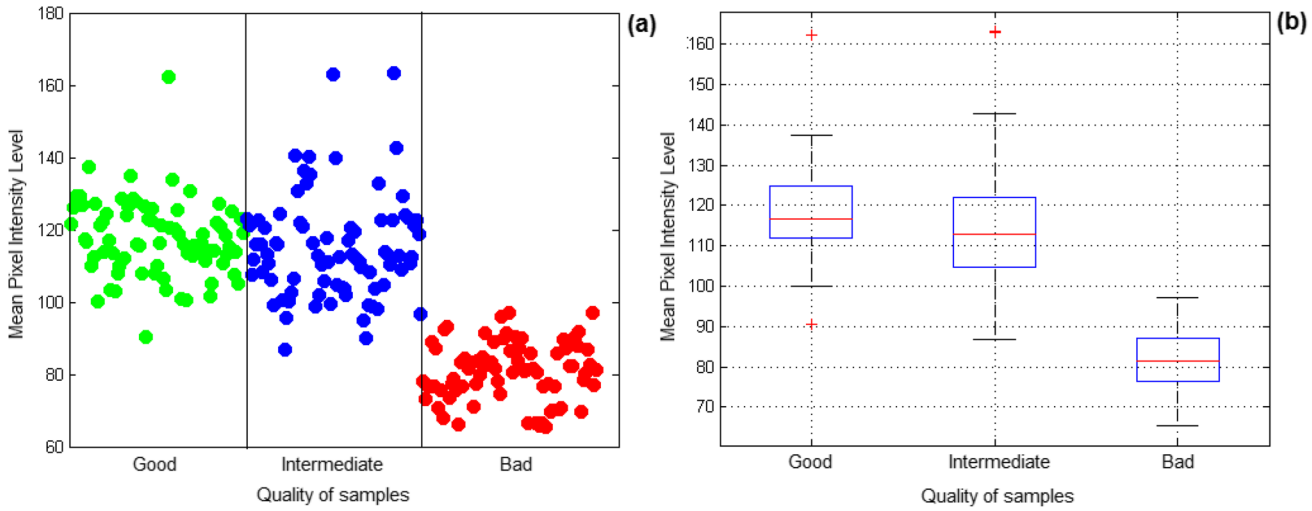

Fig. 5 Mean pixel intensity levels of green layer of the training tindora samples represented as **a** scatter diagram and **b** boxplot

quality through the intermediate phase. The good samples exhibit a more linear trend with lesser thickness, whereas in the intermediate and the bad, some tools are producing much bulkier plot. This is found as one of the key features for determining the fruit quality. But the major drawback of these plots, for the proposed quality classification, is that though these plots were sufficient enough to classify the good samples from the intermediate and bad group of samples, the intermediate and the bad samples could hardly be distinguished from the same plots with prominent efficiency. Besides, the problem lying with the direct analysis of green and red layers from the RGB colour map is that the RGB colour map has high sensitivity towards luminance of image. These intensity levels of the same sample vary to a large extent as the image is captured under diverse light intensity, as well as under sources with diverse colour temperature.

HSV Representation–Based Classification

In order to incorporate further clarity of analysis as well as to increase the classification accuracy between the intermediate and bad samples, we have chosen to inspect another colour map, which is the hue-saturation-vital component (HSV) colour map.

The hue level of the images from the HSV colour map has only been considered. Further, the mean pixel density from the hue layer for each class of the images has been computed; similar operations have been done for the green and red layers. The distribution of the intensity levels for the three classes in the form of

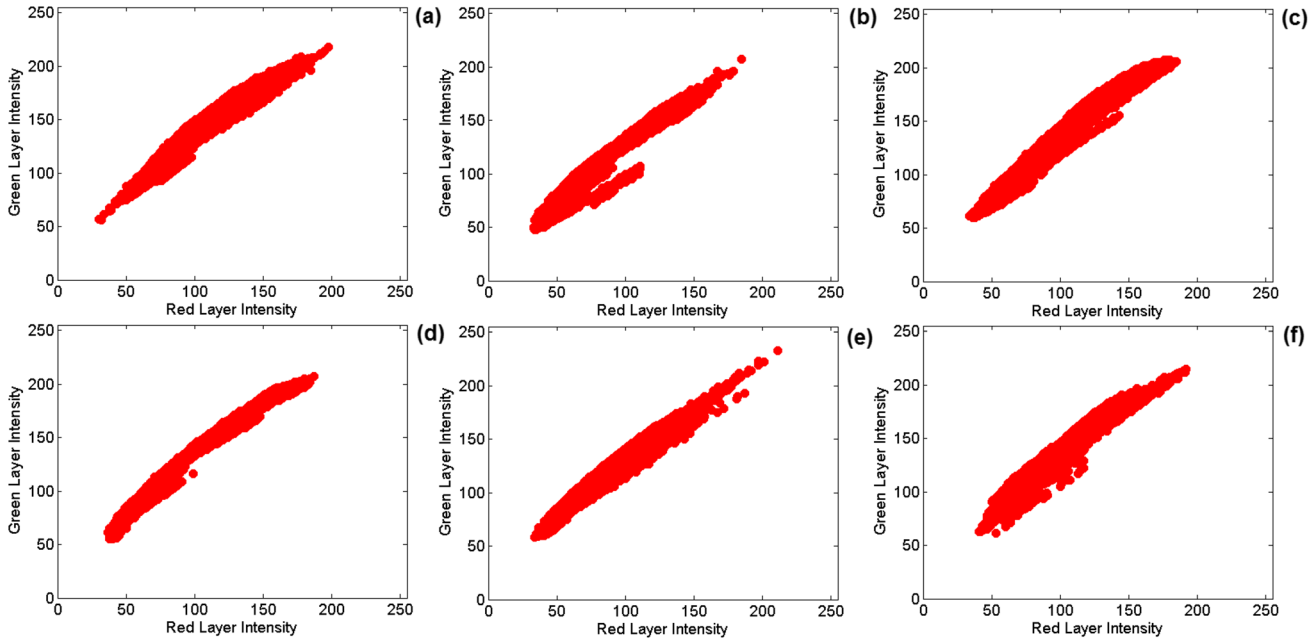

Fig. 6 Red vs. green intensity plot of a few randomly selected samples belonging to the *good* class. (**a**)–(**f**) represent intensity plot of randomly chosen sample from the good class

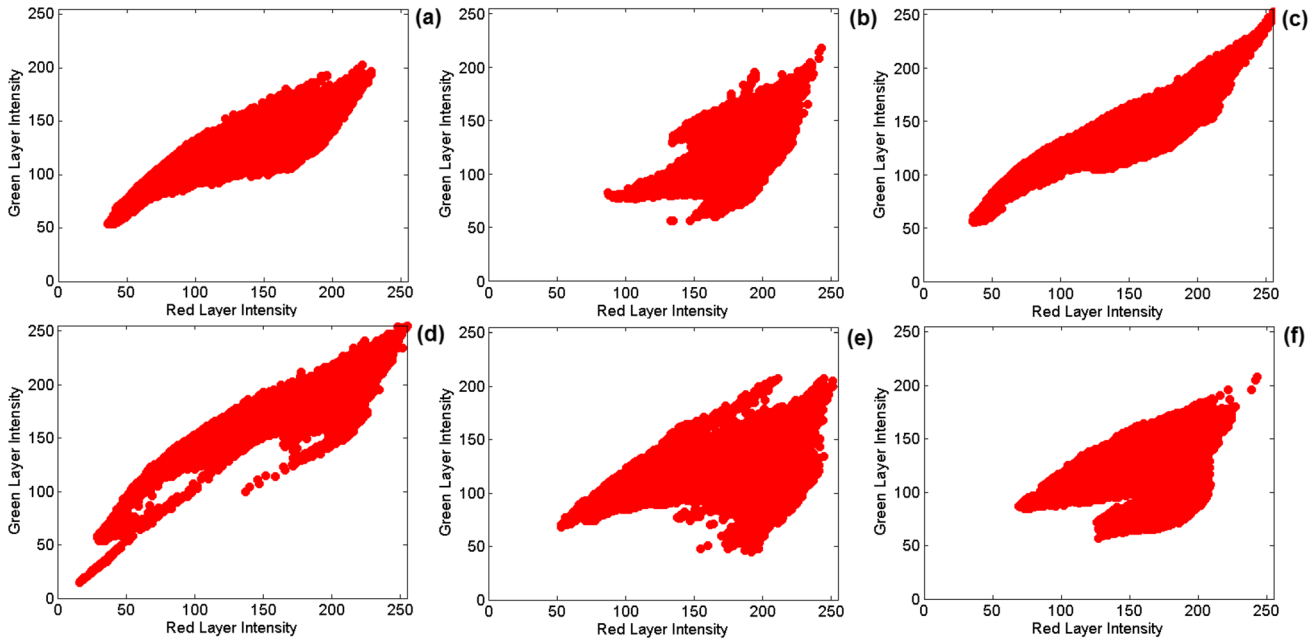

Fig. 7 Red vs. green intensity plot of a few randomly selected samples belonging to the *intermediate* class. (**a**)–(**f**) represent intensity plot of randomly chosen sample from the intermediate class

scatter plot have been shown, as well as the boxplot is developed from the same to demonstrate the diversity of the mean hue intensity level among the three classes. This is shown in Fig. 9a and b, respectively.

It has been observed that the hue level shows a more prominent distinction between the three classes yielding possible higher classification accuracy, compared to the red and the green layers, as was described in Figs. 4b and

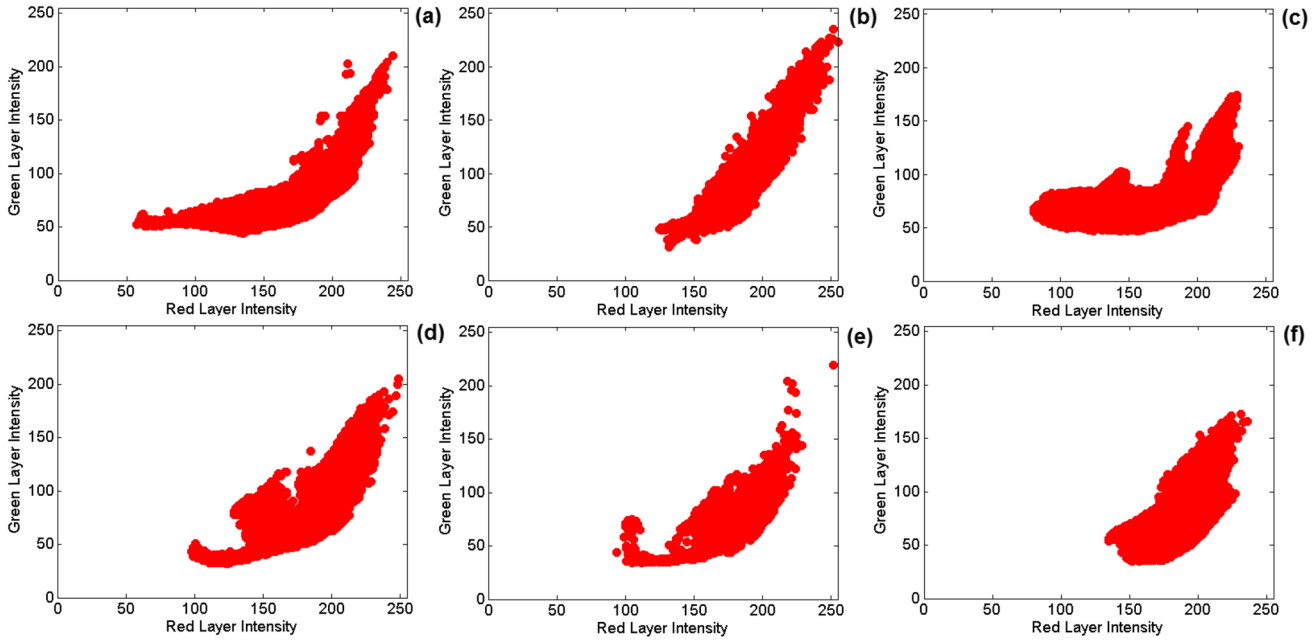

Fig. 8 Red vs. green intensity plot of a few randomly selected samples belonging to the *bad* class. (**a**)–(**f**) represent intensity plot of randomly chosen sample from the bad class

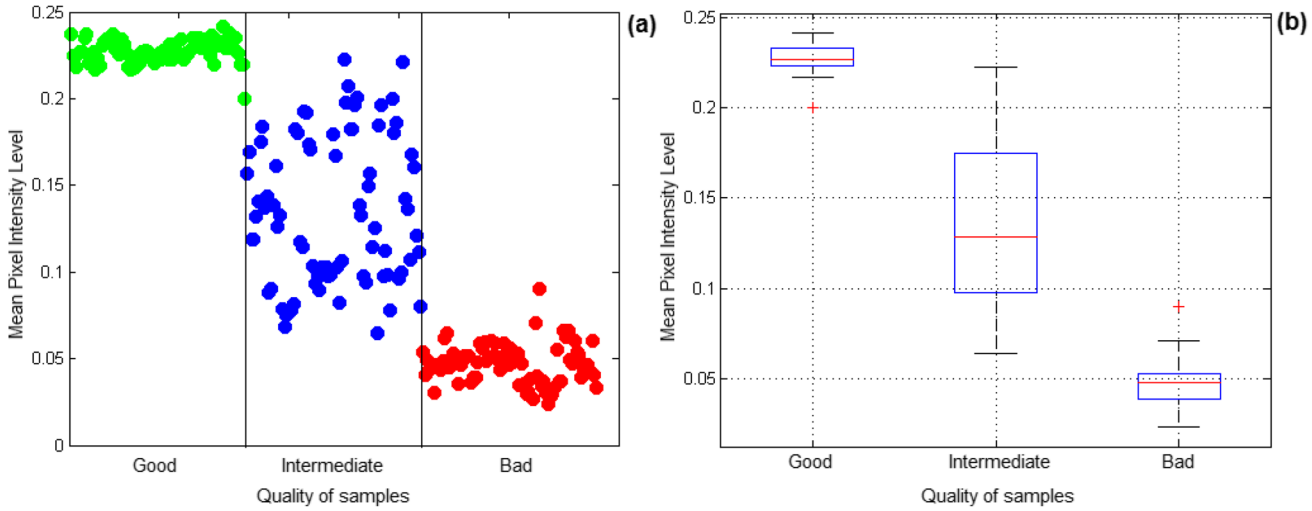

Fig. 9 Mean pixel intensity levels of hue layer of the training tindora samples represented as **a** scatter diagram and **b** boxplot

5b, respectively. This is distinctly observable, especially from the boxplot of Fig. 9b.

In order to further extract the key features of distinction between the three classes, Poincare analysis method is applied over the hue intensity layer. The hue layer is first isolated from the image, followed by converting the image matrix into its vector form. Therefore, the 100×600 image is now converted to a $60{,}000 \times 1$ vector. This conversion is done in the following way, as well as described graphically in Fig. 10:

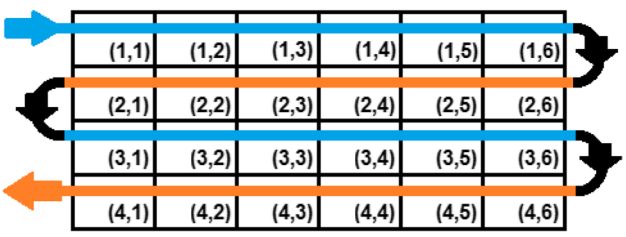

Fig. 10 Method of vectorization from image matrix

- The pixels are counted along a specific row and along the columns until the end of the image is reached.
- The row index is increased by one, followed by movement along the columns in the backward direction.
- The front column of the image is thus reached.
- This is followed by increasing the row counter once again and moving along the column in the increasing direction.
- In other words, the movement is forward and backward along the columns and along any two consecutive rows.

Application of Poincare Analysis

This deduced vector is now split into two component signals using Poincare method. This method is primarily used in abundance in the field of biomedical signal analysis and research such as ECG for the detection of abnormality in the signal. Poincare plot is basically a plot of two components of the same signal, say, *x(n)* of length *n* samples in a 2D graphical plane. The two signal components are constructed as follows:

Signal component 1, say, $x_1(n\text{-}1)$: This is developed by considering the *1st* to $(n\text{-}1)^{th}$ samples of the signal, i.e.

$$x_1(n-1) : x(1), x(2), x(3), ..., x(n-1);$$

where $x(n)$ is the original vector.

Signal component 2, say, $x_2(n\text{-}1)$: This is developed by considering the 2nd to n^{th} samples of the signal, i.e.

$$X_2(n-1) : x(2), x(3), x(4), ..., x(n);$$

where $x(n)$ is the original vector.

Thus, each component of the signal contains *(n-1)* sample points. In the proposed work, the total sample length of the image deduced vector is of 60,000; i.e. $n = 60{,}000$. Hence, each component of the signal is of length 59,999 samples. These two components are now plotted along the two axes to obtain a 2D graph. This is the Poincare plot itself. The method of development of the Poincare plot is shown in Fig. 11.

If the continuity of the signal is high, i.e. there is not much disturbance in the signal, the consecutive elements are very close to one another. In other words, the difference between the consecutive elements is very low. Thus, the trend of the Poincare plot is almost a straight line with slope close to 1. But, when a discontinuity occurs, the signal develops disturbances in the form of rapid changes in the signal level. This is duly reflected in the plot as increased randomness of the points in the vicinity of the straight line trend of the Poincare plot. Thus, the plot becomes bulkier.

Therefore, the Poincare plot is used effectively to identify major discontinuity of the signal, which primarily occurs due to large disturbances (Mukherjee et al. 2022a). In this work, it has been observed that the samples develop yellow and red zones progressively with time, whereas the tender vegetables are largely green all over the surface from one end to the other. Thus, the continuity of the green tinge gradually becomes less dominant as the samples develop yellow colouring, especially as the samples rotten. As Poincare plot is considered, which is truly the sample plot of the same but shifted signal, a cluster of points for each of the images has been obtained. Each cluster contains 59,999 sample points, refereeing to the length of the deduced Poincare component vector, which is truly the vectorized dimension of the image itself. The good class of samples produce higher levels of hue intensity and hence, are found to produce a cluster of points, almost confined in the third quadrant of the plot, whereas the bad samples produced lesser level of hue intensity and hence, are found to develop cluster in the third quadrant of the Poincare plot. Figures 12, 13 and 14 describe the Poincare plots of a random set of samples for the three classes.

Quadrant Analysis for Developing Classifier Model

In this work, 80 samples have been considered for each class to develop the training method for the classifier algorithm, whereas separate 100 samples of each class, i.e. a total of 300 samples, have been considered for validating the developed classifier. The training set of samples is used to develop the classifier and the corresponding threshold levels between each of the class boundaries by the quadrant analysis method; and the rest of the 300 samples are used to validate the proposed model.

It is well observed from the above three figures corresponding to the good, bad and intermediate class of tindora samples that the scatter points of the Poincare plot corresponding to the good class of vegetables lie mostly on the first quadrant of the figure, whereas the bad class

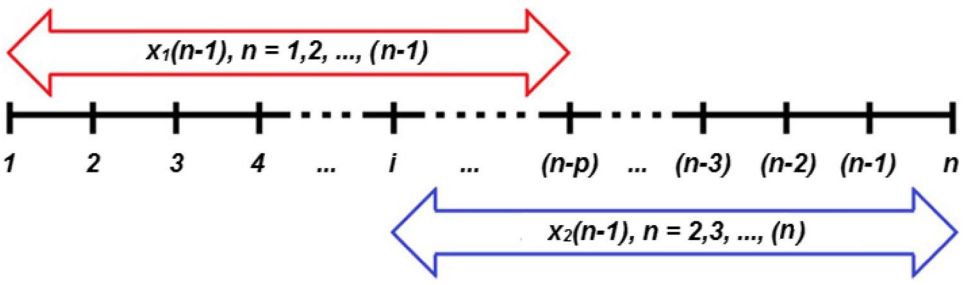

Fig. 11 Development of the Poincare plot

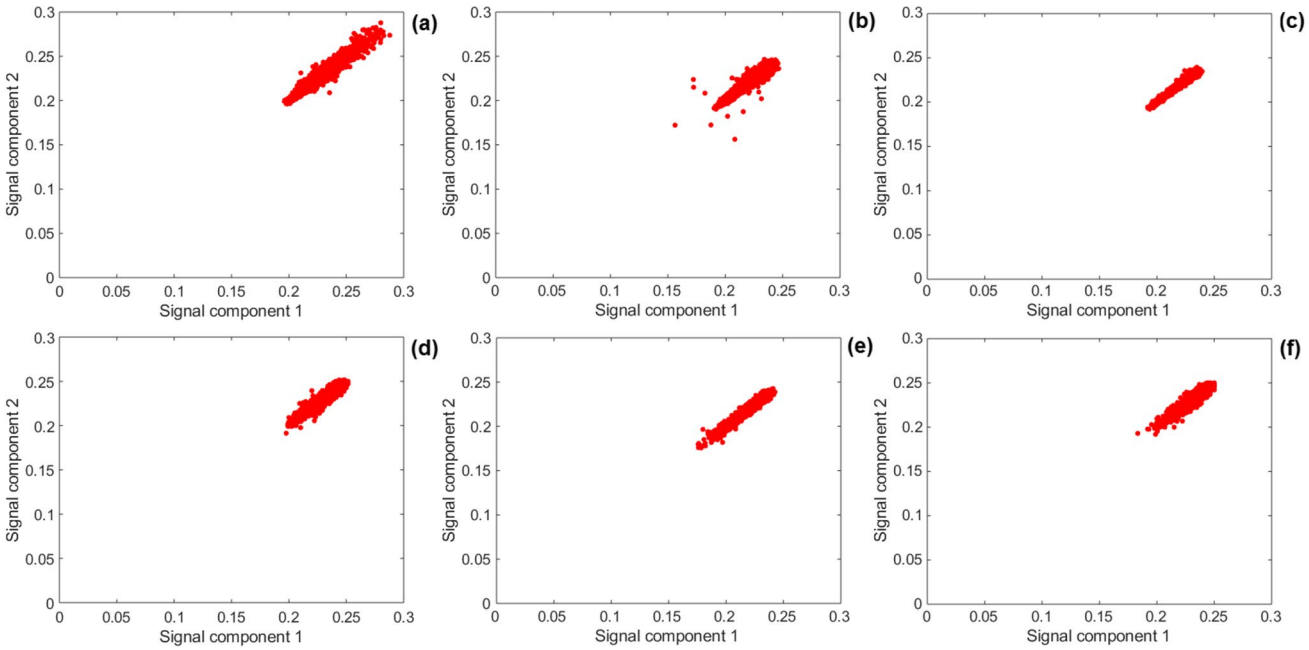

Fig. 12 Poincare plot of the *good* class of samples considering the hue intensity vector. (**a**)–(**f**) represent Poincare plot of randomly chosen sample from the good class

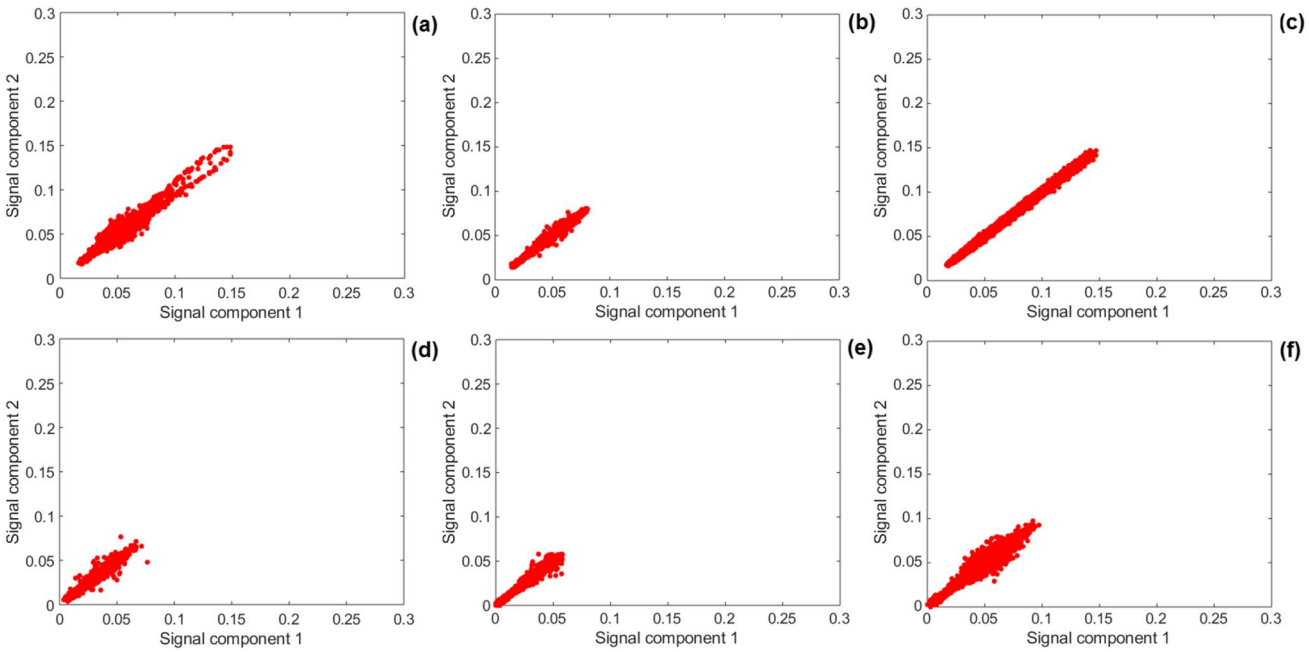

Fig. 13 Poincare plot of the *bad* class of samples considering the hue intensity vector. (**a**)–(**f**) represent Poincare plot of randomly chosen sample from the bad class

of sample mostly cluster towards the third quadrant. Intermediate samples, meanwhile, lie almost a distributed between the first and the third quadrants. Therefore, a ratio index–based analysis scheme has been developed which would compute the total number of sample points lying in the first quadrant, to the length of the vector, i.e. the total number of points in the vector. This length of the vector truly indicates the total number of pixels in the image. This ratio index has been examined, and threshold level has been designed between each of the class boundaries to separate the *good*, *intermediate* and *bad* classes of samples from each other. This index is referred to as *quadrant*

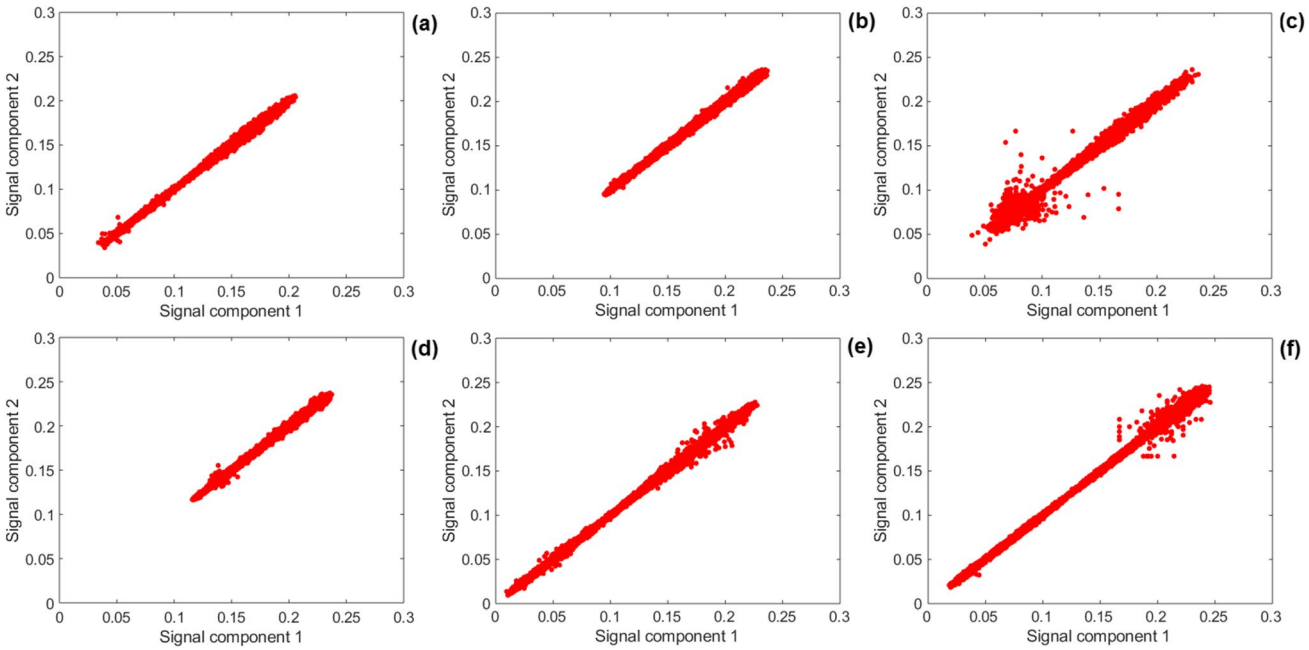

Fig. 14 Poincare plot of the *intermediate* class of samples considering the hue intensity vector. (**a**)–(**f**) represent Poincare plot of randomly chosen sample from the intermediate class

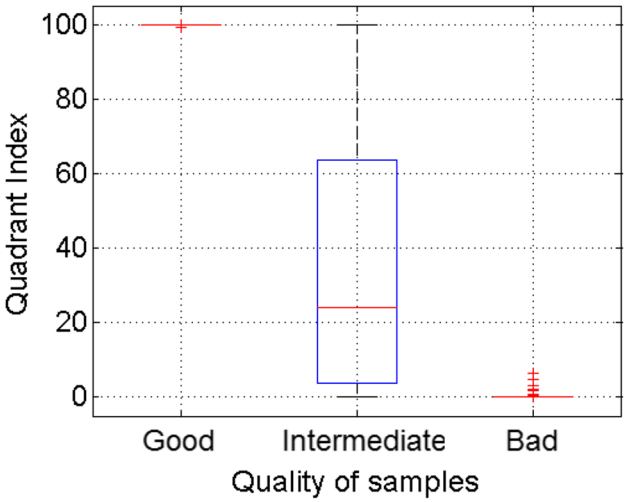

Fig. 15 Boxplot representation of the *quadrant index* of the three separate classes from Poincare quadrant analysis using the training set of samples, with 80 samples of each class

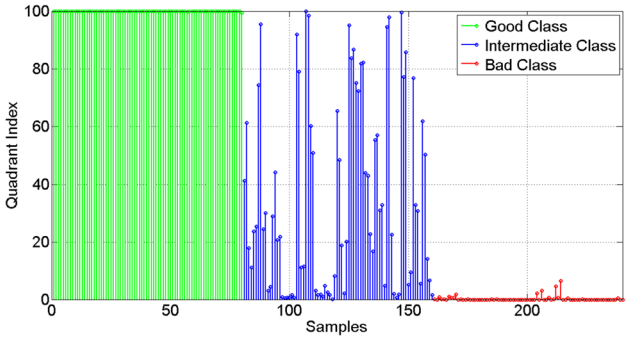

Fig. 16 Bar diagram representation of the *quadrant index* of the three separate classes from Poincare quadrant analysis using the training set of samples, with 80 samples of each class

index subsequently in the article. Thus, the *quadrant index* is defined here as:

$$QuadrantIndex(Q) = \frac{numberofpointslyinginthefirstquadrant}{totalnumberofpointsinthevector} \times 100$$

The results of classification of the samples among the *good*, *intermediate* and *bad* classes, during the development of the threshold levels of the algorithm, are described graphically in Figs. 15 to 17, where Fig. 15 describes the distribution of the *quadrant index* of the three separate classes in the form of a boxplot; Fig. 16 describes the same in the form of bar plot, where the distribution of the index of each individual sample is prominently visible; and finally, Fig. 17 describes the grouped distribution of the *quadrant index*, i.e. a histogram representation of the same results into ten different bins. These three figures clearly represent the distinct difference between the distributions of the *quadrant index* among the three classes.

Close examination of distribution of the *quadrant index* values for training phase as shown in Figs. 15 and 16 reveals that the *quadrant index* level of the *good* class of samples are close to 100% in almost all the cases, whereas the same index is close to 0% for the *bad* class of samples. The

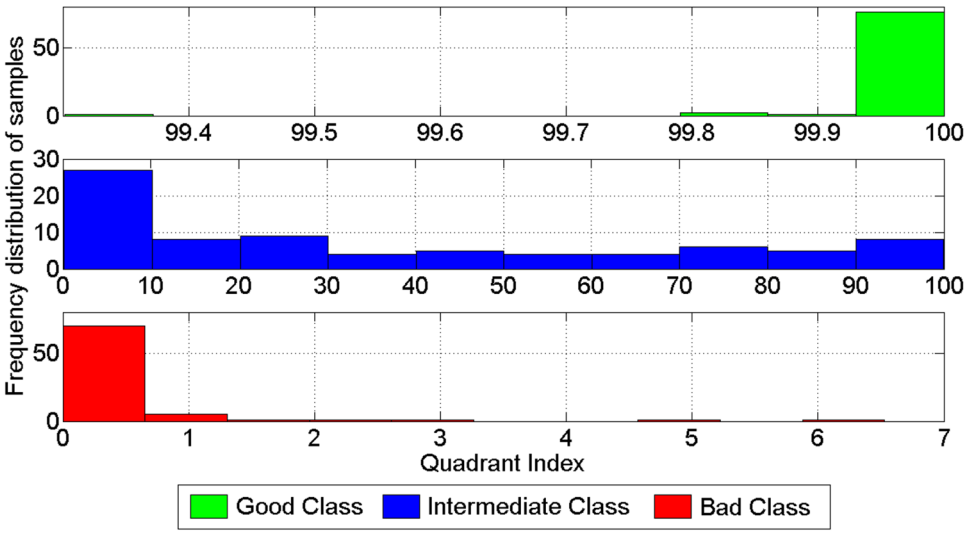

Fig. 17 Analysis of training results: Histogram representation of the *quadrant index* of the three separate classes from Poincare quadrant analysis using the training set of samples, with 80 samples of each class

quadrant index level of the *intermediate* class of samples range in between, although the difference between the *quadrant index* values for the intermediate class and good and bad class of samples, on either side of the range between 0 and 100%, is differentiable. Thus, the limiting boundary values of the quadrant indices of each class have been closely scrutinized, and two threshold limits have been developed to separate the three classes. This is done in the following way:

The mean of the lower boundary of the good class and the upper boundary of the intermediate class is computed and considered as the upper threshold limit (λ_U). From the boxplot in Fig. 15, the threshold boundary between the *good* and *intermediate* classes is obtained (see Fig. 18a, c). Similarly, the threshold boundary between *bad* and *intermediate* classes is also obtained (see Fig. 18b, d).

Result and Discussion

In this work, the classifier model using 240 samples, considering 80 samples of each class, has been designed; and testing is done using the samples from a separate dataset consisting of 300 samples, equally distributed between the three classes. It has been observed

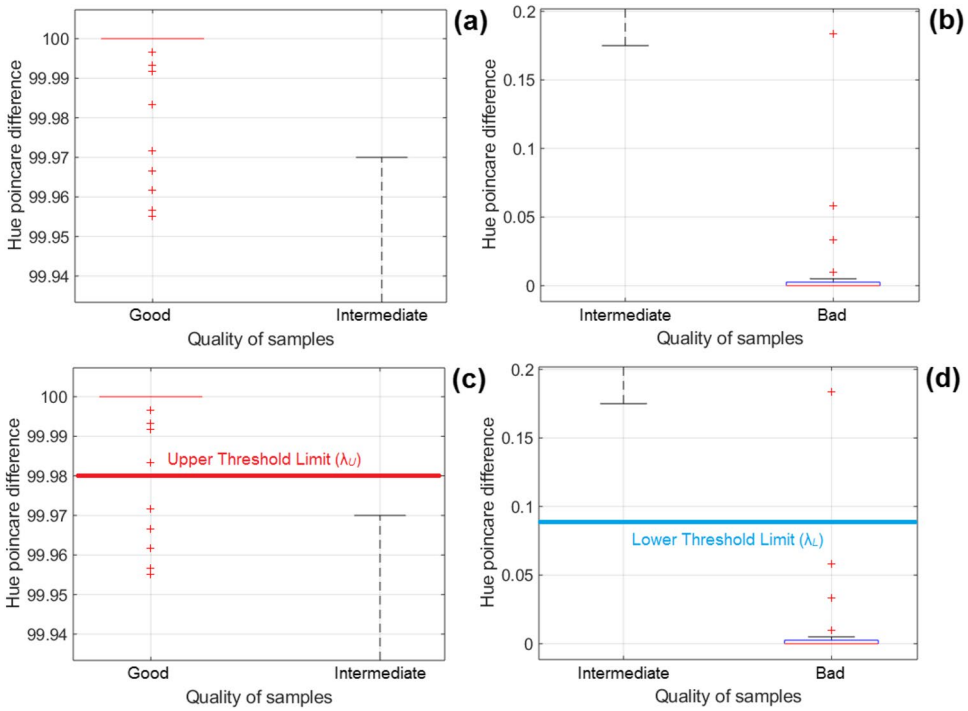

Fig. 18 Development of upper and lower threshold levels for separating the *good* and the *intermediate* classes and the *intermediate* and *bad* classes from the boxplot of Fig. 15. (**a**), (**c**) represent the boundary between good and intermediate classes, while (**b**), (**d**) represents the boundary between bad and intermediate classes

Table 2 Classifier outcomes using red layer intensity level

Quality of class		Predicted class			Total number of correct classification	Classifier accuracy (%)
		Good	Intermediate	Bad		
Actual class	Good	84	16	0	84	68.67
	Intermediate	11	56	33	56	
	Bad	0	34	66	66	

from Fig. 4b that the red layer mean intensity plot shows some minor distinctiveness among each of the three quality classes; hence, thresholds between each of the corresponding classes and a classifier scheme have been developed. Further, it is observed from the green layer mean intensity plot of Fig. 5b that there is major overlap between the consecutive freshness classes, hence bearing almost no importance in developing a robust classifier. Thus, the green layer has not been considered for any subsequent analysis. The results of the classifier using the direct threshold analysis of the red layer intensity level of Fig. 4b is shown in Table 2. It is observed from Table 2 that the accuracy of classification is below 70%, which is even below the moderate acceptable level.

This poor classification accuracy using red layer intensity level has compelled us to use hue layer analysis for developing robust and efficient classifier. Hence, the Poincare plot–based analysis of the hue intensity map of the vegetable samples has been considered. The results of the classifier using Poincare analysis of hue intensity level are shown in tabular form in Table 3, which shows a mean accuracy level of more than 94%, considering all the three freshness classes.

The results of the classifier, as observed from Table 2, show that the proposed classifier works effectively in segmentation of tindora samples into the three different classes. The overall efficiency of the classifier is found to exceed 94%, although the classification efficiency varies for individual classes.

The proposed scheme is an application of Poincare analysis which is more common practice in biomedical signal-based researches and is rarely used in food quality assessment (Sipos et al. 2017; Eftimov et al. 2020). Hence the proposed scheme shows a good application of such simple method in food quality assessment, especially for the instances where limited data point is available.

Proposed classifier produces more than 94% accuracy. The features extracted for the proposed threshold-based classifier are simple and computationally light; as a result, the proposed scheme is ideal for implementation in smartphones.

Thus, on an overall analysis, high accuracy of classification exceeding 94% level, moderate number of samples required for developing the classifier models, low intricate mathematical analysis for developing the scheme and finally, introduction of a very simple and less conventional scheme such as Poincare plot in developing equality-based 3 class classifier schemes for assessment of tindora have been the highlights of the proposed work.

Conclusion

The current work aims to construct an accurate freshness detection model for evaluating the quality of tindora samples. In this work, both the RGB and HSV representation of tindora images for quality assessment have been considered. The graphical representation of the RGB layers and the corresponding threshold classifier achieved an accuracy of 68.67% which is not acceptable. Thus, the HSV representation has been explored. The hue layer matrix was vectorized, and the Poincare plot of the vector was obtained. Quadrant analysis of the Poincare plot distribution was performed. A threshold-based classifier was designed based on the analysis. The classifier achieved an accuracy of 94.33%. The simple features and threshold-based classifiers make the proposed scheme computationally light and hence suitable for implementation in smartphones.

Table 3 Classifier outcomes using hue layer intensity level

Quality of class		Predicted class			Total number of correct classification	Classifier accuracy (%)
		Good	Intermediate	Bad		
Actual class	Good	95	5	0	95	94.33
	Intermediate	5	91	4	91	
	Bad	0	3	97	97	

Acknowledgements We acknowledge Mr. Mujtaba Siraj, final year student of department of Food Processing Technology, and Sri Snehashis Guha, PIC Malda Polytechnic, Malda, for their support to conduct this study. Thanks to GAIN (Axencia Galega de Innovación) for supporting this work (grant number IN607A2019/01).

Availability of Data and Materials Not applicable.

Code Availability Not applicable.

Declarations

Ethics Approval Not applicable.

Conflict of Interest Tanmay Sarkar declares that he has no conflict of interest. Alok Mukherjee declares that he has no conflict of interest. Kingshuk Chatterjee declares that he has no conflict of interest. Saule Ospandiyarovna Akhmetova declares that she has no conflict of interest. Aigul Surapovna Alipbekova declares that she has no conflict of interest. Marina Temerbayeva declares that she has no conflict of interest. Mohammad Ali Shariati declares that he has no conflict of interest. Maksim Rebezov declares that he has no conflict of interest. Jose Manuel Lorenzo declares that he has no conflict of interest.

References

Agudo A (2005) Measuring intake of fruit and vegetables. World Health Organization, Kobe, Japan

Akter YA, Rahman MO (2017) Development of a computer vision based eggplant grading system. In: 4th International Conference on Advances in Electrical Engineering (ICAEE). pp 285–290

Alagarraja M, Rasika T, Monika G et al (2017) Updated review on pharmacognosy, Phytochemistry and pharmacological studies of Coccinia indica. Int J Res Pharm Sci 8:54–58

Arce-Lopera C, Masuda T, Kimura A et al (2013) Luminance distribution as a determinant for visual freshness perception: evidence from image analysis of a cabbage leaf. Food Qual Prefer 27:202–207. https://doi.org/10.1016/j.foodqual.2012.03.005

Baranowski P, Mazurek W, Wozniak J, Majewska U (2012) Detection of early bruises in apples using hyperspectral data and thermal imaging. J Food Eng 110:345–355. https://doi.org/10.1016/j.jfoodeng.2011.12.038

Bhargava A, Bansal A (2021) Fruits and vegetables quality evaluation using computer vision: a review. J King Saud Univ - Comput Inf Sci 33:243–257. https://doi.org/10.1016/j.jksuci.2018.06.002

Bhaskar A, Varma S (2021) Phytochemical investigation and in vitro antioxidant activity of Coccinia grandis fruit extract. Eur J Mol Clin Med 7:3888–3894

Boyette MD, Tsirnikas AL (2017) Evaluating the shape and size characteristics of sweet potatoes using digital image analysis. 2017 ASABE Annu. Int. Meet. 1

Deng L, Du H, Han Z (2017) A carrot sorting system using machine vision technique. Appl Eng Agric 33:149–156. https://doi.org/10.13031/aea.11549

Deokate UA, Khadabadi SS (2012) Pharmacology and phytochemistry of Coccinia indica. Pharmacophore 3:179–185. https://doi.org/10.5897/JPP11.005

Dhakshina Kumar S, Esakkirajan S, Bama S, Keerthiveena B (2020) A microcontroller based machine vision approach for tomato grading and sorting using SVM classifier. Microprocess Microsyst 76:103090. https://doi.org/10.1016/j.micpro.2020.103090

Dias J (2011) World importance, marketing and trading of vegetables. Acta Hortic 921:153–169

Donis-González IR, Guyer DE (2016) Classification of processing asparagus sections using color images. Comput Electron Agric 127:236–241. https://doi.org/10.1016/j.compag.2016.06.018

Eftimov T, Popovski G, Valenčič E, Seljak BK (2020) FoodEx2vec: New foods' representation for advanced food data analysis. Food Chem Toxicol 138:111169. https://doi.org/10.1016/j.fct.2020.111169

Gunjan M, Sarangdevot YS, Vyas B (2021) Pharmacognostical study, and pharmacological review of Coccinia indica fruit and Zea mays leaves. J Pharm Sci Res 13:2021

Guzik P, Piskorski J, Krauze T et al (2006) Heart rate asymmetry by Poincaré plots of RR intervals. Biomed Tech (berl) 51:272–275. https://doi.org/10.1515/BMT.2006.054

Hadi N, Tiwari P, Singh RB et al (2022) Chapter 4 - beneficial effects of gourds in health and diseases. In: Singh RB, Watanabe S, Isaza AABT-FF and N in M and N-CD (eds) Functional foods and nutraceuticals in metabolic and non-communicable diseases. Academic Press, pp 61–77

Hendrawan Y, Rohmatulloh B, Prakoso I et al (2021) Classification of large green chilli maturity using deep learning. IOP Conf Ser Earth Environ Sci 924:12009. https://doi.org/10.1088/1755-1315/924/1/012009

Hing YS, Wan WY, Nugroho H (2021) Objective tool for chili grading using convolutional neural network and color analysis BT - advances in robotics, automation and data analytics. In: Khairuddin IM, Mohd Razman MA et al (eds) Mat Jizat JA. Springer International Publishing, Cham, pp 315–324

Hoshi RA, Pastre CM, Vanderlei LCM, Godoy MF (2013) Poincaré plot indexes of heart rate variability: relationships with other nonlinear variables. Auton Neurosci 177:271–274. https://doi.org/10.1016/j.autneu.2013.05.004

Hossain A, Maitra S (2021) Neglected and underutilized crop species: are they future smart crops in fighting poverty, hunger and malnutrition under changing climate? In: Neglected and Underutilized Crops - Towards Nutritional Security and Sustainability. Springer, pp 1–50

Hu J, Zhou C, Zhao D et al (2020) A rapid, low-cost deep learning system to classify squid species and evaluate freshness based on digital images. Fish Res 221:105376. https://doi.org/10.1016/j.fishres.2019.105376

Iwata H, Niikura S, Matsuura S et al (1998) Evaluation of variation of root shape of Japanese radish (Raphanus sativus L.) based on image analysis using elliptic Fourier descriptors. Euphytica 102:143–149. https://doi.org/10.1023/A:1018392531226

Jahanbakhshi A, Momeny M, Mahmoudi M, Radeva P (2021) Waste management using an automatic sorting system for carrot fruit based on image processing technique and improved deep neural networks. Energy Rep 7:5248–5256. https://doi.org/10.1016/j.egyr.2021.08.028

Kaur S, Girdhar A, Gill J (2018) Computer vision-based tomato grading and sorting. In: Kolhe ML, Trivedi MC, Tiwari S, Singh VK (eds) Advances in data and information sciences. Springer, Singapore, pp 75–84

Khatun S, Pervin F, Karim MR et al (2012) Phytochemical screening and antimicrobial activity of Coccinia cordifolia L. plant. Pak J Pharm Sci 25:757–761

Kondo N, Chong VK, Ninomiya K et al (2013) Application of NIR-color CCD camera to eggplant grading machine. ASAE Meet Present 300:1–9. https://doi.org/10.13031/2013.19606

Koyama K, Tanaka M, Cho B-H et al (2021) Predicting sensory evaluation of spinach freshness using machine learning model and digital images. PLoS One 16:e0248769

Lalji C, Pakrashi D, Smyth R (2018) Can eating five fruit and veg a day really keep the doctor away? Econ Model 70:320–330. https://doi.org/10.1016/j.econmod.2017.07.024

Li B, Lecourt J, Bishop G (2018) Advances in Non-destructive early assessment of fruit ripeness towards defining optimal time of harvest and yield prediction-a review. Plants (basel, Switzerland) 7:3. https://doi.org/10.3390/plants7010003

Londhe D, Nalawade S, Pawar G et al (2013) Grader: a review of different methods of grading for fruits and vegetables. Agric Eng Int CIGR J 15:217–230

McDonald LS, Panozzo JF, Salisbury PA, Ford R (2016) Discriminant analysis of defective and non-defective field pea (Pisum sativum L.) into broad market grades based on digital image features. PLoS One 11:e0155523

Mourot L, Bouhaddi M, Perrey S et al (2004) Quantitative Poincaré plot analysis of heart rate variability: effect of endurance training. Eur J Appl Physiol 91:79–87. https://doi.org/10.1007/s00421-003-0917-0

Mukherjee A, Sarkar T, Chatterjee K (2021) Freshness assessment of Indian gooseberry (Phyllanthus emblica) using probabilistic neural network. J Biosyst Eng. https://doi.org/10.1007/s42853-021-00116-8

Mukherjee A, Chatterjee K, Kundu PK, Das A (2022a) Application of Poincaré analogous time-split signal-based statistical correlation for transmission line fault classification. Electr Eng 104:1057–1075. https://doi.org/10.1007/s00202-021-01369-4

Mukherjee A, Sarkar T, Chatterjee K et al (2022c) Development of artificial vision system for quality assessment of oyster mushrooms. Food Anal Methods. https://doi.org/10.1007/s12161-022-02241-2

Mukherjee A, Chatterjee K, Sarkar T (2022b) Entropy-aided assessment of amla (Emblica officinalis) quality using principal component analysis. Biointerface Res Appl Chem 12:2162–2170. https://doi.org/10.33263/BRIAC122.21622170

Navotas IC, Santos CNV, Balderrama EJM et al (2018) Fish identification and freshness classification through image processing using artificial neural network. ARPN J Eng Appl Sci 18:4912–4922

Otoya PEL, Gardini SRP (2021) A machine vision system based on RGB-D image analysis for the artichoke seedling grading automation according to leaf area. In: IEEE 3rd Eurasia Conference on IOT, Communication and Engineering (ECICE). pp 176–181

Pfeiffer WH, McClafferty B (2007) HarvestPlus: breeding crops for better nutrition. Crop Sci 47:S-88-S-105. https://doi.org/10.2135/cropsci2007.09.0020IPBS

Pietro CD, Cefola M, Pace B et al (2018) Non-destructive automatic quality evaluation of fresh-cut iceberg lettuce through packaging material. J Food Eng 223:46–52. https://doi.org/10.1016/j.jfoodeng.2017.11.042

Przybylak A, Kozłowski R, Osuch E et al (2020) Quality evaluation of potato tubers using neural image analysis method. Agric 10:112. https://doi.org/10.3390/agriculture10040112

Raikar MM, Meena SM, Kuchanur C et al (2020) Classification and grading of okra-ladies finger using deep learning. Procedia Comput Sci 171:2380–2389. https://doi.org/10.1016/j.procs.2020.04.258

Rong D, Xie L, Ying Y (2019) Computer vision detection of foreign objects in walnuts using deep learning. Comput Electron Agric 162:1001–1010. https://doi.org/10.1016/j.compag.2019.05.019

Ropelewska E, Szwejda-Grzybowska J (2021) A comparative analysis of the discrimination of pepper (Capsicum annuum L.) based on the cross-section and seed textures determined using image processing. J Food Process Eng 44:e13694. https://doi.org/10.1111/jfpe.13694

Sakharkar P, Chauhan B (2017) Antibacterial, antioxidant and cell proliferative properties of Coccinia grandis fruits. Avicenna J Phytomedicine 7:295–307

Sarkar T, Mukherjee A, Chatterjee K (2021a) Supervised learning aided multiple feature analysis for freshness class detection of Indian gooseberry (Phyllanthus emblica). J Inst Eng Ser A. https://doi.org/10.1007/s40030-021-00585-2

Sarkar T, Mukherjee A, Chatterjee K et al (2021b) Comparative analysis of statistical and supervised learning models for freshness assessment of oyster mushrooms. Food Anal Methods. https://doi.org/10.1007/s12161-021-02161-7

Sarkar T, Mukherjee A, Chatterjee K et al (2022) Edge detection aided geometrical shape analysis of Indian gooseberry (Phyllanthus emblica) for freshness classification. Food Anal Methods. https://doi.org/10.1007/s12161-021-02206-x

Shahin A, Tollner W, Gitaitis D et al (2002) Classification of sweet onions based on internal defects using image processing and neural network techniques. Trans ASAE 45:1613. https://doi.org/10.13031/2013.11046

Singh B (2021) Vegetables: source of adequate health. Ann Hortic 13:124–130. https://doi.org/10.5958/0976-4623.2020.00023.7

Sipos L, Ladányi M, Gere A et al (2017) Panel performance monitoring by Poincaré plot: a case study on flavoured bottled waters. Food Res Int 99:198–205. https://doi.org/10.1016/j.foodres.2017.04.029

Su Q, Kondo N, Li M et al (2018) Potato quality grading based on machine vision and 3D shape analysis. Comput Electron Agric 152:261–268. https://doi.org/10.1016/j.compag.2018.07.012

Su Q, Kondo N, Al Riza DF, Habaragamuwa H (2020) Potato quality grading based on depth imaging and convolutional neural network. J Food Qual 2020:8815896. https://doi.org/10.1155/2020/8815896

Tamilselvan N, Thirumalai T, Elumalai EK et al (2011) Pharmacognosy of Coccinia grandis: a review. Asian Pac J Trop Biomed 1:S299–S302. https://doi.org/10.1016/S2221-1691(11)60176-7

Tu K, Ren K, Pan L, Li H (2007) A study of broccoli grading system based on machine vision and neural networks. In: 2007 International Conference on Mechatronics and Automation. pp 2332–2336

Valous NA, Mendoza F, Sun DW, Allen P (2009) Texture appearance characterization of pre-sliced pork ham images using fractal metrics: Fourier analysis dimension and lacunarity. Food Res Int 42:353–362. https://doi.org/10.1016/J.FOODRES.2008.12.012

Wargovich MJ (2000) Anticancer properties of fruits and vegetables. HortScience 35:573–575. https://doi.org/10.21273/hortsci.35.4.573

Yuniarti W, Sumardjo W, Wibawa WD (2022) Development of highland vegetable commodity areas through multi-criteria decision making (MCDM) analysis and geographic information systems. IOP Conf Ser Earth Environ Sci 950:12074. https://doi.org/10.1088/1755-1315/950/1/012074

Zhou C, Hu J, Xu Z et al (2020) A monitoring system for the segmentation and grading of broccoli head based on deep learning and neural networks. Front Plant Sci 11.https://doi.org/10.3389/fpls.2020.00402